On the ignition characteristics of NH_3/air and NH_3/H_2/air mixing layers in turbulent flows

Se Young Oh and Chun Sang Yoo
Department of Mechanical Engineering, Ulsan National Institute of Science and Technology
Ulsan, Republic of Korea

1 Abstract

The effects of turbulence on the ignition characteristics of NH_3/air and NH_3/H_2/air mixing layers are investigated using direct numerical simulations (DNS) with a detailed chemistry under elevated pressure conditions. 1-D simulations are conducted to understand the role of the scalar dissipation rate in NH_3/air and NH_3/H_2/air mixing layers. The result shows that the ignition of NH_3/air mixing layer is delayed with decreasing the mixing layer thickness or increasing the characteristic scalar dissipation rate. For NH_3/H_2/air mixing layers, however, the ignition is advanced in time with increasing the characteristic scalar dissipation rate. 2-D DNSs are performed to investigate the effects of turbulence on ignition delay of the mixing layers. In general, the ignition is assisted by low intensity turbulence regardless of the hydrogen content ratio. However, high intensity turbulence retards the ignition of the NH_3/air mixing layer, while advancing in time the ignition of the NH_3/H_2/air mixing layer, exhibiting different impact on the ignition characteristics. It is also observed that the flame propagation after ignition is disturbed by the high intensity turbulence regardless of the hydrogen content ratio.

2 Introduction

In recent years, ammonia ($\mathbf{NH_3}$) has attracted increasing attention as a clean alternative to fossil fuels. Its carbon free nature is one of the important factors for the usage of ammonia. From the combustion point of view, however, ammonia has several challenges such as low burning velocity, narrow flammability range and high auto-ignition temperature. Thus, the addition of $\mathbf{H_2}$ has been regarded as one of the solutions to promote ammonia combustion. The ignition delay of $\mathbf{NH_3}$/air mixture, which is one of the most important combustion characteristics for designing industrial devices such as internal combustion engines and gas turbine combustors, significantly decreases with the addition of $\mathbf{H_2}$ [1].

In practical operating conditions, turbulent flow has been generally observed. Due to the complicated interaction between turbulence and chemical reactions, many researchers have studied the effects of turbulence on the ignition of various fuel/air mixtures [2,3]. Basically, it has been found that turbulence assists auto-ignition by generating the locally lowest scalar dissipation rate region, which suppresses heat and radical losses. For high intensity turbulence, however, the ignition delay was found to be

Correspondence to: csyoo@unist.ac.kr

retarded [2]. However, the detailed investigation of these contrary effects of turbulence on ignition delay has not be performed. Furthermore, only a few studies have been conducted to investigate the effects of turbulence on the combustion of $\mathbf{NH_3}$/air and $\mathbf{NH_3}$/$\mathbf{H_2}$/air mixing layers [4].

The objective of the present research is thus to understand the effects of turbulence on ignition characteristics of NH_3/air and NH_3/H_2/air mixing layers at relatively high and low turbulence intensities under high pressure condition of 10 atm by performing direct numerical simulations (DNS) of the interaction between turbulence and chemical reactions in 2-D mixing layers with a detailed chemistry. Ignition delay is defined by the chemical explosive mode analysis which is effective and convenient method to measure ignition delay and localize ignition kernel in the mixing layer.

3 Numerical Setup and Initial Conditions

A series of DNSs are conducted to investigate the ignition characteristics of 2-D NH_3/air and NH_3/H_2/air mixing layers in a turbulent flow by using Sandia DNS code, S3D, which solves the compressible Navier-Stokes, continuity equations together with the species and energy equations. An eight-order central finite difference scheme is used for spatial derivatives, and a fourth-order and six-stage explicit Runge-Kutta method is applied for time intengation. A detailed chemical mechanism (San Diego mechanism) is used, involving 19 spcies and 64 reaction steps [5].

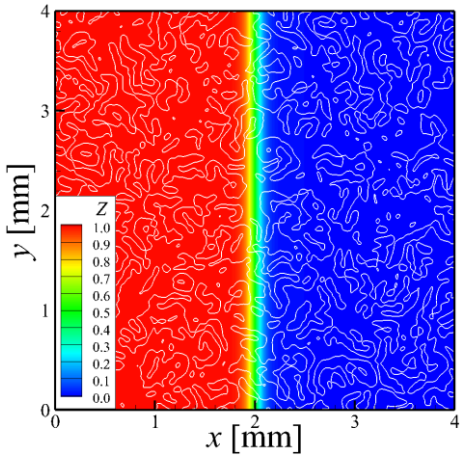

Figure 1: Initial mixture fraction contour and isolines of the specific velocity magnitude (white solid lines).

Figure 1 shows the initial mixture fraction contour field including the isoline of velocity magnitude. The mixture fraction, *Z*, is equal to 1 and 0 in the fuel and oxidizer sides, respectively. Along the *x*-direction, stratified scalar fields such as species mass fraction and temperature are initialized as:

$$\phi(x) = \phi_{air} + \frac{\phi_{fuel} - \phi_{air}}{2}\left(\tanh\left(\frac{x + L/2}{\sigma}\right) - \tanh\left(\frac{x - L/2}{\sigma}\right)\right) \quad (1)$$

where ϕ_{fuel} and ϕ_{air} are the scalar values in the fuel and oxidizer sides, respectively. L is the width of the domain in the *x*-direction, 4 mm, and σ the constant for the mixing layer thickness. Temperature of fuel, T_{fuel}, is set to 400 K, and temperature of air, T_{air}, is varied to match the same 1-D laminar ignition delay (50 μs) at 10 atm according to the hydrogen content ratio, R_{H2}, which is defined as $X_{\mathrm{H2}}/(X_{\mathrm{NH3}} + X_{\mathrm{H2}})$ to investigate the rate of change of ignition delay affected by turbulence as

compared to the 1-D ignition delay. Non-reflecting and periodic boundary conditions are applied on each side in *y*- and *x*- direction, respectively [6,7].

The homogeneous isotropic turbulent velocity field is initialized using the Passot-Pouquet spectrum [8]. Table 1 shows the detailed turbulent parameters including the 1-D stoichiometric laminar flame speed (S_L) and flame thickness (D_f) scales according to R_{H2}. S_L is calculated by CHEMKIN, and D_f is described as $(T_b - T_u)/(\nabla T)_{max}$, where T_b and T_u are temperature of burned and unburned gas, respectively.

Table 1: Turbulent parameters for initial conditions including the characteristics scale of flame speed and length.

Case	R_{H2}	S_L(cm/s)	D_f(mm)	l_t(mm)	l_t/D_f	$\tau_{ig,1D}(\mu s)$	$(l_t/u^{'})/\tau_{ig,1D}$	Re_{turb}
1	0.0	6.90	0.279	0.558	2.0	50	1.0	448
2	0.0	6.90	0.279	0.558	2.0	50	2.0	224
3	0.0	6.90	0.279	0.558	2.0	50	4.0	112
4	0.1	8.69	0.236	0.472	2.0	50	1.0	320
5	0.1	8.69	0.236	0.472	2.0	50	2.0	160
6	0.1	8.69	0.236	0.472	2.0	50	4.0	80

Integral length scale, l_t, is set to match $l_t/D_f = 2$. RMS turbulent fluctuation velocity, u', is varied to match $(l_t/u')/\tau_{ig,1D} = 1, 2$ and 4 to modify the ratio of turbulence and chemical time scales. Ignition delay is defined by the chemical explosive mode analysis (CEMA). Detailed information on CEMA can be found in [9]. Thus, ignition delay is the time when λ_{exp}, which is the largest eigenvalue of the Jacobian matrix of the chemical source term, becomes the negative value.

4 Results and Discussion

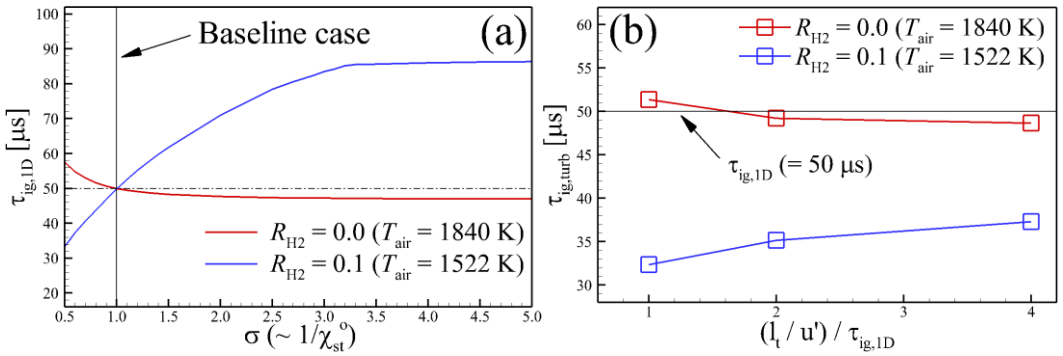

Figure 2: (a) 1-D ignition delays as a function of σ in the 1-D laminar mixing layer and (b) 2-D ignition delays as a function of normalized turbulence time scale, $(l_t/u')/\tau_{ig,1D}$, of 2-D DNS cases.

It is necessary to investigate the variation in the ignition delay according to the mixing layer thickness represented as the characteristic scalar dissipation rate, χ_{st}^{o}, which is the scalar dissipation rate measured at the stoichiometric mixture fraction line in the initial field. This is because the ignition delay is affected by the fluctuation of χ along the most reactive mixture fraction [2]. Figure 2a shows the variation in the

ignition delay in 1-D laminar mixing layer as a function of σ in Eq. (1) at $R_{\mathrm{H2}} = 0.0$ and 0.1. Note that the mixing layer thickness is inversely proportional to χ_{st}^{o}. For pure ammonia with $R_{\mathrm{H2}} = 0.0$, the ignition delay decreases with increasing σ or decreasing χ_{st}^{o}. For $R_{\mathrm{H2}} = 0.1$, however, the ignition delay shows an opposite trend to the variation in χ_{st}^{o}; the ignition delay increases with increasing σ or decreasing χ_{st}^{o}. This reult shows that the effect of the variation in χ_{st}^{o} on the ignition delay can be varied by R_{H2}.

Figure 2b shows the variation in the ignition delay as a function of normalized turbulent time scale, defined as the ratio of turbulent time scale (l_t/u') to chemical time scale ($\tau_{ig,1D}$), or $(l_t/u')/\tau_{ig,1D}$ for 2-D DNS cases. It is readily observed that in general, turbulent flow advances the ignition in time, compared to that in 1-D cases at relatively low intensity regardless of R_{H2}. With the increase of turbulence intensity, however, the ignition for $R_{\mathrm{H2}} = 0.0$ is retarded in time by turbulence and as such, its ignition delay becomes larger than $\tau_{ig,1D}$ of 50 μs at $(l_t/u')/\tau_{ig,1D} = 1.0$. In contrast, the ignition delay for $R_{\mathrm{H2}} = 0.1$ continuously decreases with increasing the turbulence intensity. However, 2-D ignition delay for $R_{\mathrm{H2}} = 0.1$ is much smaller than the corresponding 1-D ignition delay. The advance of the ignition delay in 2-D cases is primarily attributed to the effect of the differential diffusion of hydrogen, which will be further investigated in the future study.

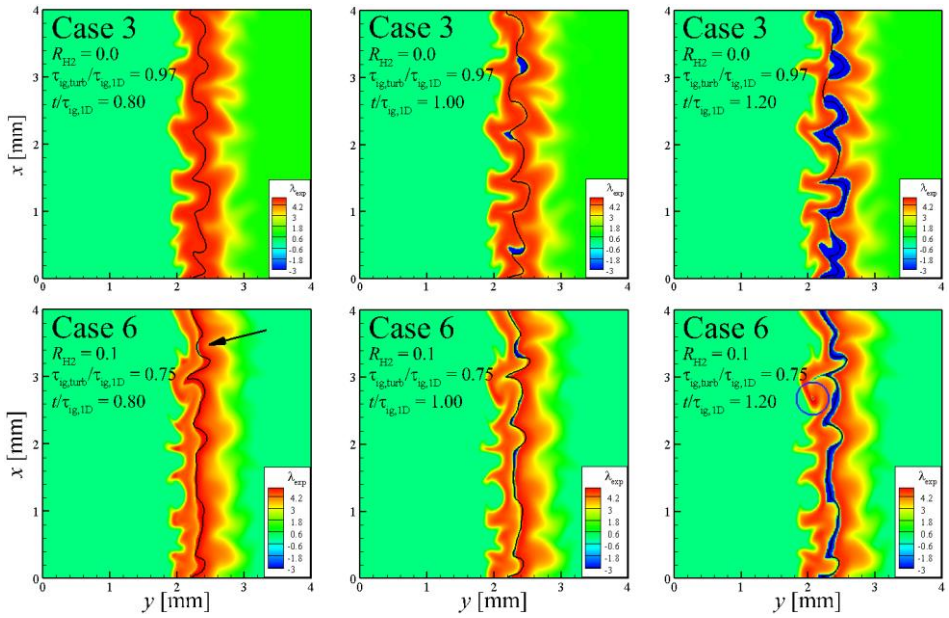

Figure 3: Isocontours of λ_{exp} at low turbulent intensity for Cases 3 and 6.

To further identify the turbulence effect on the ignition characteristics, the temporal evolution of λ_{exp} isocontours for Cases 3 and 6 are shown in Fig. 3, which represent low turbulence intensity cases. Black solid lines in Fig. 3 represent the isoline of the most reactive mixture fraction that are Z = 0.0028 and 0.0032 for $R_{\mathrm{H2}} = 0.0$ and 0.1, respectively. For Case 3, it is readily observed that the ignition first occurs at both concave and convex regions on the most reactive mixture fraction isoline. These ignition kernels locally propagate towards the surroundings. For Case 6, the ignition characteristics become different from those for Case 3. Once an ignition kernel is first generated (see the black arrow), ignition kernels develop spontaneously along the most reactive mixture fraction line. In addition, another ignition kernel is generated at a relatively fuel-rich mixture (see the blue circle).

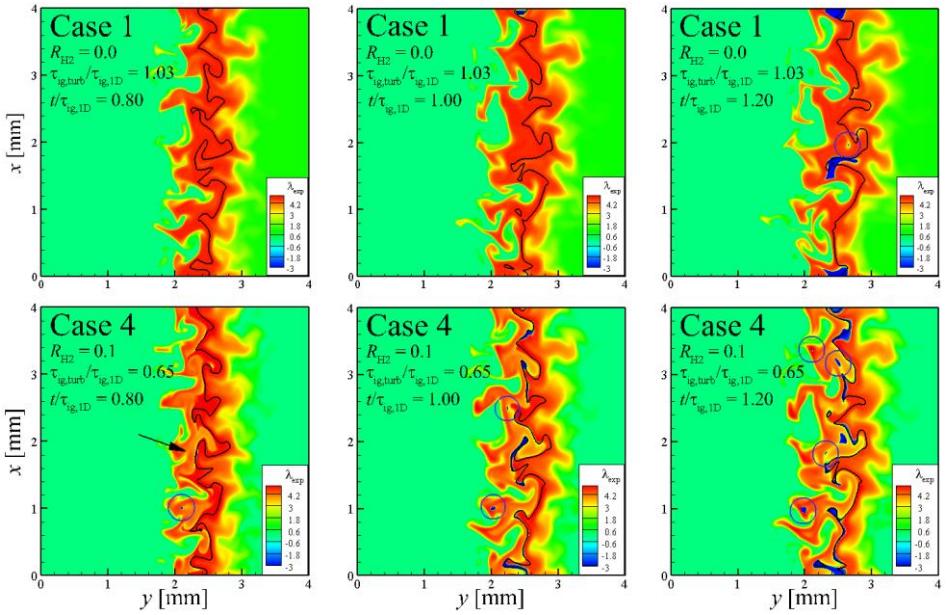

Figure 4: Isocontours of λ_{exp} at the high turbulent intensity (Case 1 and case 4).

Figure 4 shows the temporal evolution of λ_{exp} isocontours for Cases 1 and 4, which represent high turbulence intensity cases. For Case 1, it is readily observed that ignition and propagation are retarded by high intensity turbulence. In addition, ignition kernels are found to develop in relatively rich mixture similar to that in Case 6. Although the first ignition kernel for Case 4 develops faster than those of the other cases as shown in Fig 2, its propagation is disturbed by high intensity turbulence. In the future study, the ignition and flame propagation characteristics will be further investigated.

Acknowledgement

This work was supported by Basic Science Research Program through the National Research Foundation of Korea (NRF) funded by the Ministry of Science and ICT (NRF-2021R1A2C2005606).

References

[1] J. Otomo, M. Koshi, T. Mitsumori, H. Iwasaki, K. Yamada (2018). Chemical kinetic modeling of ammonia oxidation with improved reaction mechanism for ammonia/air and ammonia/hydrogen/air combustion. Int. J. Hydrog. Energy. 43: 3004.

[2] E. Mastorakos, T. A. Baritaud, T. J. Poinsot (1997). Numerical simulations of autoignition in turbulent mixing flows. Combust. Flame. 109: 198.

[3] Z. Li, X. Gou, Z. Chen. (2019). Effects of hydrogen addition on non-premixed ignition of iso-octane by hot air in a diffusion layer. Combust. Flame. 199: 292.

[4] W. Yang, K. K. R. Dinesh, K. H. Luo, D. Thevenin (2022). Direct numerical simulations of auto-igniting mixing layers in ammonia and ammonia-hydrogen combustion under engine-relevant conditions. Int. J. Hydrog. Energy. 47: 38055.

[5] Y. Jiang, A. Gruber, K. Seshadri, F. Williams (2020) An updated short chemical-kinetic igniting nitrogen mechanism for carbon-free combustion applications. Int. J. Energy Res. 44: 795.

[6] C. S. Yoo, Y. Wang, A. Trouve, H. G. Im (2005) Characteristic boundary conditions for direct simulations of turbulent counterflow flames. Combust. Theory Model. 9: 617-546.

[7] C. S. Yoo, H. G. Im (2007) Characteristic boundary conditions for simulations of compressible reacting flows with multi-dimensional, viscous and reaction effects. Combust. Theory Model. 11: 259-286.

[8] T. Passot, A. Pouquet (1987) Numerical simulation of compressible homogeneous flows in the turbulent regime. J. Fluid Mech. 181: 441

[9] Z. Luo, C. S. Yoo, E. S. Richardson, J. H. Chen, C. K. Law, T. Lu (2012) Chemical explosive mode analysis for a turbulent lifted ethylene jet flame in highly-heated coflow. Combust. Flame. 159: 265.